2019 27th Mediterranean Conference on Control and Automation (MED)
July 1–4, 2019 · Akko · Israel

Temporal Circular Formation Control with Bounded Trajectories in a Uniform Flowfield

Anoop Jain and Daniel Zelazo

Abstract— **This paper studies circular formation control of multi-vehicle systems, modeled with unicycle dynamics, in a uniform flowfield with different temporal phase arrangements, while assuring that the trajectories of the vehicles remains bounded within a region. Using the idea of *Barrier Lyapunov function* in conjunction with temporal phase potential functions, we derive control laws that achieves our objectives, under a mild assumption on the initial states of the vehicles. We further obtain bounds on the various signals in the post-design analysis and show that these depends on the initial conditions and controller gains. Simulations are provided to illustrate the theoretical findings.**

Index Terms— **Multi-agent systems, cooperative control, nonlinear control, stabilization, Barrier Lapunov Function.**

I. Introduction

Formation control of multi-agent systems has been a widely researched topic in the last decade [1]. Several formation patterns are explored in the literature in different practical contexts, while circular formation control has received considerable attention because of its applications in both natural and man made systems. Foraging ants around a sugar piece, a swirlingly growing epiphyte colony, and schooling of fish around a predator are some of the examples from natural systems [2]. Examples from engineering applications are tracking, source seeking, capturing, monitoring and securing a target or a search region [3]–[9]. Inspired by these, the present work studies the problem of circular formation control of a team of unmanned vehicles such as unmanned aerial vehicles (UAVs) or autonomous underwater vehicles (AUVs) that are deployed for surveillance, tracking or monitoring missions.

One of the important requirements in such applications is that the motion trajectories of the vehicles remains confined to a given workspace. For instance, while carrying out surveillance operations across the territories of two countries, it is required that the trajectories of the unmanned vehicles do not cross the boundaries due to security purposes. On the other hand, trajectory-constrained motion offers an additional advantage of maintaining connectivity of the group such that there is no risk of loosing any vehicle due to sensor limitations, which, in turn, shows faster convergence of underlying distributive control laws. Besides, there are several other applications where trajectory-constrained motion has been of a great importance for instance, cooperative space missions where it is desired that the spacecrafts do not cross the earth's environment [10].

The authors are with the Faculty of Aerospace Engineering, Israel Institute of Technology, Haifa 32000, Israel (e-mail: anoopjain.jn@gmail.com; dzelazo@technion.ac.il). This work was supported in part by Lady Davis Fellowship and the German-Israeli Foundation for Scientific Research and Development.

Other risky factors that may cause an unmanned vehicle to move outside the restricted region is the disturbance from an external source−for instance, wind in case of UAVs operation. Thus, it is important to assure trajectory-constrained cooperative control of multi-agent (or multi-vehicle) systems in presence of any external disturbance.

The present work considers this problem where our objective is to stabilize temporal phase arrangements in a team of UAVs, modeled with unicycle dynamics, around a desired common circle with bounded trajectories in the presence of a uniform wind flow. Stabilization of temporal collective formation is particularly important in applications where an area under inspection is required to be monitored in regular time intervals. Note that the main intent of the paper is to emphasize the trajectory-constrained aspect of the formation control problems; other complex flow properties are not considered in this work for simplicity. The reader may refer [11] for a discussion about various flows and their properties.

The concept of Control Barrier Function (CBF) is one of the modern control design tools for solving the problem of stabilization, without violating the system's constraints [12], [13]. Recently, CBF is widely used in the study of multi-agent systems [14]–[17]. *Barrier Lyapunov Function* (BLF) is a special class of CBF, which becomes unbounded when approaches to the boundary limits. Two types of BLFs are generally seen in the literature−Logarithmic BLF [18] and Tangent BLF [19]. In this paper, we use the idea of Logarithmic BLF as introduced in [18] to solve the problem considered in this paper.

The main contributions of this work are as follows:

1) Unlike [11], we consider that the vehicles are moving with heterogeneous constant speeds in a uniform flowfield and interact using limited motion information.
2) By exploiting the idea of BLF, we propose the stabilizing controllers that asymptotically stabilize a fleet of vehicles to a desired common circle in temporal phase patterns of two-types, namely temporal phase synchronization and balancing.
3) We further obtain bounds on the various signals in the post-design analysis and show that these depends on the initial conditions and controller gains.

Note that, in an earlier work [20], only the trajectory-constrained aspect was addressed and the effect of external disturbance was not incorporated.

The paper is organized as follows: Section II describes the vehicle model in a uniform flowfield and reviews some preliminary results related to BLF. Section III introduces potential functions to stabilize collective circular motion with temporal phase arrangements. Section IV derives control laws, obtains bound on various intermediate signals and

978-1-7281-2803-0/19/$31.00 ©2019 IEEE

discusses a simulation example. We conclude the paper in Section V with some future directions of the research.

Notations: $\mathbb{R}$, $\mathbb{C}$, and $\mathbb{R}_+$ denotes the set of real numbers, complex numbers and nonnegative real numbers, respectively. The set $\mathbb{S}^1$ denotes the unit circle. The $N-$torus is the Cartesian product $\mathbb{T}^N = \mathbb{S}^1 \times \ldots \times \mathbb{S}^1$ ($N-$times). For a complex number $z \in \mathbb{C}$, $\Re(z)$ and $\Im(z)$ are its real part and imaginary part, and $\bar{z}$ is the complex conjugate of z. The inner product $\langle z_1, z_2 \rangle$ of two complex numbers $z_1, z_2 \in \mathbb{C}$ is defined as $\langle z_1, z_2 \rangle = \Re(\bar{z}_1 z_2)$. For vectors $\boldsymbol{w}_1 \in \mathbb{C}^N$ and $\boldsymbol{w}_2 \in \mathbb{C}^N$, the inner product is defined as $\langle \boldsymbol{w}_1, \boldsymbol{w}_2 \rangle = \Re(\boldsymbol{w}_1^\star \boldsymbol{w}_2)$, where $\boldsymbol{w}^\star$ represents the conjugate transpose of $\boldsymbol{w}$. Let $\mathfrak{D} \subseteq \mathbb{R}^N$ and $f : \mathfrak{D} \to \mathbb{R}$ be a differential map. Then ∇f is the gradient of f, that is, $\nabla f = \text{grad} f = \left[\frac{\partial f}{\partial x_1}, \ldots, \frac{\partial f}{\partial x_N}\right]^T$. The vectors $\mathbf{0}_N$ and $\mathbf{1}_N$ are used to represented by $\mathbf{0}_N = [0, 0, \ldots, 0]^T \in \mathbb{R}^N$, and $\mathbf{1}_N = [1, 1, \ldots, 1]^T \in \mathbb{R}^N$, respectively.

A graph is a pair $\mathcal{G} = (\mathcal{V}, \mathcal{E})$, which consist a finite set of vertices $\mathcal{V}$ and undirected edges $\mathcal{E} \subset \mathcal{V} \times \mathcal{V}$. The Laplacian of a graph $\mathcal{G}$, denoted by $\mathcal{L} \in \mathbb{R}^{|\mathcal{V}| \times |\mathcal{V}|}$, is defined as: $[\mathcal{L}]_{jk} = |\mathcal{N}_j|$ for $j = k$, $[\mathcal{L}]_{jk} = -1$ for $k \in \mathcal{N}_j$, $[\mathcal{L}]_{jk} = 0$ otherwise, where $|\mathcal{N}_j|$ is the cardinality of the set $\mathcal{N}_j$. The incidence matrix $\mathcal{B} \in \mathbb{R}^{|\mathcal{V}| \times |\mathcal{E}|}$ of graph $\mathcal{G}$ with an arbitrary orientation is defined such that for edge $\ell = (j, k) \in \mathcal{E}$ (where $j \in \mathcal{V}$ is the head and $k \in \mathcal{E}$ is the tail of edge ℓ), $[\mathcal{B}]_{j\ell} = +1$, $[\mathcal{B}]_{k\ell} = -1$, and $[\mathcal{B}]_{m\ell} = 0$ for $m \neq j, k$. For an undirected and connected graph, Laplacian $\mathcal{L}$ (i) is symmetric and positive semi-definite; (ii) has an eigenvalue of zero associated with the eigenvector $\mathbf{1}_N$, that is, $\mathcal{L}\boldsymbol{x} = 0_N$ iff $\boldsymbol{x} = \mathbf{1}_N x_0$; (iii) $\mathcal{L} = \mathcal{B}\mathcal{B}^T$. A graph $\mathcal{G}$ is circulant if and only if its Laplacian $\mathcal{L}$ is a circulant matrix, that is, $\mathcal{L}$ is completely defined by its first row [21].

II. System Model and Preliminaries

A. System Model

The motion of nonholonomic vehicles such as UAV or AUV can be modeled by a unicycle model. We consider a group of N vehicles, where the equations of motion of the k^{th} vehicle are given by

$$\dot{x}_k = v_k \cos\theta_k \tag{1a}$$
$$\dot{y}_k = v_k \sin\theta_k \tag{1b}$$
$$\dot{\theta}_k = u_k, \quad k = 1, \ldots, N, \tag{1c}$$

where (x_k, y_k) are the positional coordinates of the vehicle in a planar space, v_k is the linear speed, θ_k is the heading angle, and u_k is the control law to be designed in order to accomplish the objective of this paper. If control input u_k is identically zero for all k, all the vehicles move along the straight lines with slopes $\theta_k(0)$. On the other hand, if $u_k = \omega_k \neq 0$ is a constant, all the vehicles move along respective circular path of radius $\rho_k = v_k/|\omega_k|$, where the direction of rotation along the circle is determined by using the convention that $\omega_k > 0$ for the anticlockwise movement, while $\omega_k < 0$ for the clockwise movement. For the sake of simplicity, we identify the $\mathbb{R}^2$ plane with a complex plane $\mathbb{C}$ and describe the equations of motions (1) in terms of the complex number $i = \sqrt{-1}$ as:

$$\dot{r}_k = v_k e^{i\theta_k} \tag{2a}$$
$$\dot{\theta}_k = u_k, \quad k = 1, \ldots, N, \tag{2b}$$

where $e^{i\theta_k} = \cos\theta_k + i\sin\theta_k$ is known as Euler's formula and r_k is the position of the k^{th} vehicle.

B. Flowfield and Modified System Model

Flowfield is an external disturbance which may severely affect the motion of the vehicles aimed for some cooperative task. Depending upon various operating conditions, the flowfield may have very chaotic properties. However, in this paper, we consider the case of a time-invariant uniform flowfield for the sake of clarity, which could be extended to time varying case as in [11]. Let the uniform flowfield at any point in the space be given by $f = \lambda e^{i\mu}$, where $|f| = |\lambda|$ is the strength of the flowfield in the direction μ and satisfies the assumption that $|\lambda| < \min_k v_k, \forall k$. This assumption ensures that a vehicle can always make forward progress as measured in an inertial frame. Thus, the equations of motion of the k^{th} vehicle in the flowfield are

$$\dot{r}_k = v_k e^{i\theta_k} + f \tag{3a}$$
$$\dot{\theta}_k = u_k(\boldsymbol{r}, \boldsymbol{\theta}), \quad k = 1, \ldots, N. \tag{3b}$$

Let $s_k = |v_k e^{i\theta_k} + f|$ be the magnitude of the resultant velocity vector and $\gamma_k = \arg(v_k e^{i\theta_k} + f)$ be the resultant heading angle of the k^{th} vehicle in the inertial frame. Then, the motion equations (3) in the inertial frame can be expressed as:

$$\dot{r}_k = s_k e^{i\gamma_k} \tag{4a}$$
$$\dot{\gamma}_k = \zeta_k(\boldsymbol{r}, \boldsymbol{\gamma}), \quad k = 1, \ldots, N, \tag{4b}$$

where ζ_k is the control input in the inertial frame. Note that $s_k \geq v_k - |\lambda| \geq 0$ for all k, according to our assumption on the flowfield f. The applied control u_k in terms of the inertial speed s_k and heading angle γ_k can be obtained as follows:

$$s_k \sin\gamma_k = v_k \sin\theta_k + \langle f, i \rangle \tag{5a}$$
$$s_k \cos\gamma_k = v_k \cos\theta_k + \langle f, 1 \rangle, \tag{5b}$$

from which, we have that

$$\tan\gamma_k = \frac{v_k \sin\theta_k + \langle f, i \rangle}{v_k \cos\theta_k + \langle f, 1 \rangle}. \tag{6}$$

Taking the time-derivative of the above equation and using the fact that $\langle f, 1 \rangle = \lambda\cos\mu$ and $\langle f, i \rangle = \lambda\sin\mu$, yields:

$$\dot{\gamma_k} = \frac{v_k^2 + v_k\lambda\cos\mu\cos\theta_k + v_k\lambda\sin\mu\sin\theta_k}{(1 + \tan^2\gamma_k)(v_k\cos\theta_k + \lambda\cos\mu)^2}\dot{\theta}_k$$

Substituting for $\tan^2\gamma_k$ from (6), along with $v_k\sin\theta_k = s_k\sin\gamma_k - \lambda\sin\mu$ and $v_k\cos\theta_k = s_k\cos\gamma_k - \lambda\cos\mu$ from (5), we have:

$$u_k = \frac{v_k^2 - \lambda^2 + 2\lambda s_k\cos(\mu - \gamma_k)}{v_k^2 - \lambda^2 + \lambda s_k\cos(\mu - \gamma_k)}\zeta_k, \tag{7}$$

which could be further simplified by substituting for speed s_k. The speed s_k of the k^{th} vehicle in the inertial frame is given by

$$\begin{aligned} s_k &= |v_k e^{i\theta_k} + \lambda e^{i\mu}| \\ &= \sqrt{(v_k \cos\theta_k + \lambda\cos\mu)^2 + (v_k \sin\theta_k + \lambda \sin\mu)^2} \\ &= \sqrt{v_k^2 + \lambda^2 + 2\lambda v_k \cos(\mu - \theta_k)}. \end{aligned}$$

Squaring on both sides and substituting θ_k in terms of γ_k as done above, we get

$$s_k^2 - 2\lambda s_k \cos(\mu - \gamma_k) + \lambda^2 - v_k^2 = 0, \tag{8}$$

which gives

$$s_k = \lambda\cos(\mu - \gamma_k) + \sqrt{v_k^2 - \lambda^2 \sin^2(\mu - \gamma_k)}. \tag{9}$$

From (7) and (8), it yields that

$$u_k = \frac{\zeta_k}{1 - \lambda s_k^{-1}\cos(\mu - \gamma_k)}, \tag{10}$$

which is well defined due to our assumption that $|\lambda| < \min_k v_k$ for all $k = 1, \ldots, N$. These expressions will be used in sequel to derive further results in this paper.

C. Barrier Lyapunov Function

This subsection reviews some preliminary results related to BLF.

Definition 1 ([18]). *A Barrier Lyapunov Function is a scalar function $V(\boldsymbol{x})$ of state vector $\boldsymbol{x} \in \mathcal{D}$, defined with respect to the system $\dot{\boldsymbol{x}} = f(\boldsymbol{x})$ on an open region $\mathcal{D}$ containing the origin, that is continuous, positive definite, has continuous first-order partial derivatives at every point of $\mathcal{D}$, has the property $V(\boldsymbol{x}) \to \infty$ as $\boldsymbol{x}$ approaches the boundary of $\mathcal{D}$, and satisfies $V(\boldsymbol{x}(t)) \leq \beta, \forall t \geq 0$, along the solution of $\dot{\boldsymbol{x}} = f(\boldsymbol{x})$ for $\boldsymbol{x}(0) \in \mathcal{D}$ and some positive constant β.*

Lemma 1 ([18]). *For any positive constant c, let $\mathcal{Z} := \{\xi \in \mathbb{R} : -c < \xi < c\} \subset \mathbb{R}$ and $\mathcal{N} := \mathbb{R}^\ell \times \mathcal{Z} \subset \mathbb{R}^{\ell+1}$ be open sets. Consider the system $\dot{\boldsymbol{\eta}} = \boldsymbol{h}(t, \boldsymbol{\eta})$, where, $\boldsymbol{\eta} := [\boldsymbol{w}, \xi]^T \in \mathcal{N}$, and $\boldsymbol{h} : \mathbb{R}_+ \times \mathcal{N} \to \mathbb{R}^{\ell+1}$ is piecewise continuous in t and locally Lipschitz in $\boldsymbol{\eta}$, uniformly in t, on $\mathbb{R}_+ \times \mathcal{N}$. Suppose that there exist functions $U : \mathbb{R}^\ell \to \mathbb{R}_+$ and $V_1 : \mathcal{Z} \to \mathbb{R}_+$, continuously differentiable and positive definite in their respective domains, such that $V_1(\xi) \to \infty$ as $|\xi| \to c$ and $\gamma_1(\|\boldsymbol{w}\|) \leq U(\boldsymbol{w}) \leq \gamma_2(\|\boldsymbol{w}\|)$, where, γ_1 and γ_2 are class $\mathcal{K}_\infty$ functions. Let $V(\boldsymbol{\eta}) \triangleq V_1(\xi) + U(\boldsymbol{w})$, and $\xi(0) \in \mathcal{Z}$. If it holds that $\dot{V} = (\nabla V)^T \boldsymbol{h} \leq 0$, in the set $\xi \in \mathcal{Z}$, then $\xi(t) \in \mathcal{Z}, \ \forall t \in [0, \infty)$.*

In the sequel, we use these results to prove some theoretical results in this paper.

III. Trajectory-Constrained Collective Circular Formation with Temporal Phase Arrangements

A. Trajectrory-Constrained Collective Circular Formation

The circular formation of the group of vehicles is characterized by their motion along the same desired circular orbit. By saying the *desired* circle we mean that the center and radius of the circle can be chosen to the desired values,

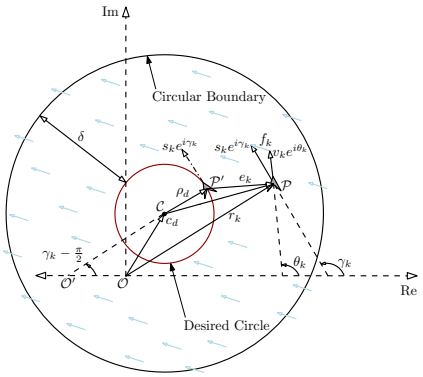

Fig. 1. Motion of the k^{th} vehicle on the desired common circle in flowfield.

depending upon an application. The scenario is shown in Fig. 1, where it is required that all the vehicles must move on a desired circle of radius ρ_d and center at c_d. In order to achieve the motion around the same circle, we would like to minimize the error e_k as shown in Fig. 1, which is obtained using vector parallelogram rule as:

$$e_k = (r_k - c_d) + i\rho_d e^{i\gamma_k}. \tag{11}$$

Denoting $\boldsymbol{e} = [e_1, \ldots, e_N]^T$ as the error vector, we consider the following potential function,

$$\mathcal{S}(\boldsymbol{e}) = \mathcal{S}(\boldsymbol{r}, \boldsymbol{\gamma}) \triangleq \frac{1}{2}\sum_{k=1}^{N} \ln\left(\frac{\delta^2}{\delta^2 - |e_k|^2}\right), \tag{12}$$

where '$\ln(\cdot)$' denotes the natural logarithmic and $\delta > 0$ is a constant, which could be appropriately chosen to restrict vehicles' trajectories to lie within a predefined circular boundary at all times. The potential $\mathcal{S}(\boldsymbol{r}, \boldsymbol{\gamma})$ is positive semi-definite and continuously differentiable for $|e_k| < \delta, \forall k$ and becomes zero whenever $e_k = 0$ for all k [18]. This means that the minimization of $\mathcal{S}(\boldsymbol{r}, \boldsymbol{\gamma})$ corresponds to the situation when all the vehicles move on the desired common circle, that is, $e_k = 0$ implies

$$r_k = c_d - i\rho_d e^{i\gamma_k}, \ \forall k, \tag{13}$$

which is the position of the k^{th} vehicle on the desired circle (see Fig. 1). The time derivative of the potential function $\mathcal{S}(\boldsymbol{e})$ along the system dynamics (4) is

$$\dot{\mathcal{S}} = \frac{1}{2}\sum_{k=1}^{N}\left(\frac{\delta^2 - |e_k|^2}{\delta^2}\right)\left(\frac{\delta^2(\frac{d}{dt}|e_k|^2)}{(\delta^2 - |e_k|^2)^2}\right) = \sum_{k=1}^{N}\frac{\frac{1}{2}\frac{d}{dt}|e_k|^2}{\delta^2 - |e_k|^2}.$$

The term $\frac{1}{2}\frac{d}{dt}|e_k|^2$ can be obtained as follows:

$$\frac{1}{2}\frac{d}{dt}|e_k|^2 = \frac{1}{2}\frac{d}{dt}\langle e_k, e_k\rangle = \frac{1}{2}\left(\langle e_k, \dot{e}_k\rangle + \langle \dot{e}_k, e_k\rangle\right) = \langle e_k, \dot{e}_k\rangle.$$

Substituting for e_k from (11), along with the fact that $\rho_d = s_k/\omega_k$, yields $\frac{1}{2}\frac{d}{dt}|e_k|^2 = \langle r_k - c_d + i\rho_d e^{i\gamma_k}, \dot{r}_k - \rho_d e^{i\gamma_k}\dot{\gamma}_k\rangle = \langle r_k - c_d + i\rho_d e^{i\gamma_k}, s_k e^{i\gamma_k} - s_k e^{i\gamma_k}\frac{\zeta_k}{\omega_k}\rangle = \langle r_k - c_d + i\rho_d e^{i\gamma_k}, e^{i\gamma_k}\rangle\left(1 - \frac{\zeta_k}{\omega_k}\right)s_k = \left(\langle r_k - c_d, e^{i\gamma_k}\rangle + \langle i\rho_d e^{i\gamma_k}, e^{i\gamma_k}\rangle\right)\left(1 - \frac{\zeta_k}{\omega_k}\right)s_k = \langle r_k - c_d, e^{i\gamma_k}\rangle\left(1 - \frac{\zeta_k}{\omega_k}\right)s_k$, as $\langle i\rho_d e^{i\gamma_k}, e^{i\gamma_k}\rangle = 0$. Thus,

$$\dot{\mathcal{S}} = \sum_{k=1}^{N}\frac{\langle r_k - c_d, e^{i\gamma_k}\rangle}{\delta^2 - |e_k|^2}\left(1 - \frac{\zeta_k}{\omega_k}\right)s_k. \tag{14}$$

B. Temporal Synchronization and Balancing Phase Patterns

Along with the trajectory-constrained motion around the desired common circle, one would also like to achieve other formation control objectives assigned to the vehicle's group. In this direction, in this subsection, we achieve various temporal phase patterns of the vehicles' motion around the desired common circle. Note that since all the vehicles are moving with constant speed with respect to the flowfield, spatial phase patterns may not be controllable [20].

Recall from Subsection II-B that the speed of the vehicle k depends upon the resultant heading γ_k in the flowfield, that is, $s_k = s(\gamma_k)$ as v_k is fixed for each vehicle. Moreover, differentiating (11) gives $\dot{e}_k = (s_k - \rho_d\dot{\gamma}_k)e^{i\gamma_k}$. Substituting $\dot{\gamma}_k = (1/\rho_d)s_k$ ensures $\dot{e}_k = 0$, which implies that the k^{th} vehicle traverses a circle of radius ρ_d. Integrating control $\dot{\gamma}_k = (1/\rho_d)s_k$, using separation of variables, yields

$$t = \rho_d \int_0^{\gamma_k(t)} \frac{d\gamma}{s(\gamma)}. \tag{15}$$

According to [11], we can use the quantity at the RHS of (15) as a measure of the temporal separation of solutions to (4). Defining

$$T = \rho_d \int_0^{2\pi} \frac{d\gamma}{s(\gamma)} > 0 \tag{16}$$

as the time period of single revolution, we define the time phase ψ_k as

$$\psi_k = \frac{2\pi\rho_d}{T} \int_0^{\gamma_k} \frac{d\gamma}{s(\gamma)}. \tag{17}$$

The time-derivative of (17) along the solutions of (4) is given by

$$\dot{\psi}_k = \frac{2\pi}{T}\rho_d s_k^{-1}\zeta_k. \tag{18}$$

Let $\mathcal{U}(\boldsymbol{\psi}) := \frac{N}{2}|p_\psi|^2$ be a temporal phase potential function, where $p_\psi := \frac{1}{N}\sum_{j=1}^{N} e^{i\psi_j}$ is the centroid of the temporal phase unit vectors $e^{i\psi_k}$, $k = 1, \ldots, N$. Note that the magnitude $|p_\psi|$ satisfies $0 \leq |p_\psi| \leq 1$ and hence $0 \leq \mathcal{U}(\boldsymbol{\psi}) \leq N/2$. Furthermore, $\mathcal{U}(\boldsymbol{\psi})$ is rotationally invariant, that is, $\mathcal{U}(\boldsymbol{\psi} + \psi_0\mathbf{1}) = \mathcal{U}(\boldsymbol{\psi}), \psi_0 \in \mathbb{S}^1$, and achieves its maximum value if $\psi_1 = \ldots = \psi_N$, that is called temporal phase synchronization. While the minimization of $\mathcal{U}(\boldsymbol{\psi})$ achieves when $p_\psi = 0$, which we call as temporal phase balancing.

Definition 2 (*Temporal Phase Synchronization and Balancing*)**.** *The temporal synchronized and balanced phase patterns corresponds to the arrangements of temporal phases $\boldsymbol{\psi} = [\psi_1, \ldots, \psi_N]^T$ such that $|p_\psi| = 1$ and $p_\psi = 0$, respectively.*

To incorporate limited communication constraints among vehicles, as will be discussed later, the potential $\mathcal{U}(\boldsymbol{\psi})$ can be further modified. Following [4], [21], for undirected and time-invariant communication, we achieve temporal phase synchronization and balancing by optimizing the potential function

$$\mathcal{W}(\boldsymbol{\psi}) = \frac{1}{2}\langle e^{i\boldsymbol{\psi}}, \mathcal{L}e^{i\boldsymbol{\psi}}\rangle, \tag{19}$$

which is a Laplacian quadratic form associated with temporal phasors $e^{i\boldsymbol{\psi}} = [e^{i\psi_1}, \ldots, e^{i\psi_N}]^T$, and is positive semi-definite. Note that, for a connected graph, the quadratic form (19) vanishes only when $e^{i\boldsymbol{\psi}} = e^{i\psi_0}\mathbf{1}_N$, where $\psi_0 \in \mathbb{S}^1$ is a constant, that is, the potential $\mathcal{W}(\boldsymbol{\psi})$ is minimized in the temporal synchronized phase arrangements. Additionally, if the graph is circulant, temporal phase balancing corresponds to the maximization of $\mathcal{W}(\boldsymbol{\psi})$, which is summarized in the following lemma.

Lemma 2 ([4], [21])**.** *Let $\mathcal{L}$ be the Laplacian of an undirected and connected graph $\mathcal{G} = (\mathcal{V}, \mathcal{E})$ with N vertices. Consider the Laplacian phase potential $\mathcal{W}(\boldsymbol{\psi})$ defined in* (19)*. If $e^{i\boldsymbol{\psi}}$ is an eigenvector of $\mathcal{W}(\boldsymbol{\psi})$, then $\boldsymbol{\psi}$ is a critical point of $\mathcal{W}(\boldsymbol{\psi})$, and $\boldsymbol{\psi}$ is either temporal phase synchronized or balanced in the sense of Definition 2. The potential $\mathcal{W}(\boldsymbol{\psi})$ reaches its global minimum if and only if $\boldsymbol{\psi}$ is synchronized. If $\mathcal{G}$ is circulant, then $\mathcal{W}(\boldsymbol{\psi})$ reaches its global maximum $\frac{N}{2}\sigma_{max}$ in temporal balanced phase arrangement, where σ_{max} is the maximum eigenvalue of $\mathcal{L}$.*

The time derivative of $\mathcal{W}(\boldsymbol{\psi})$, along the dynamics (4), is

$$\dot{\mathcal{W}} = \sum_{k=1}^{N}\left(\frac{\partial\mathcal{W}}{\partial\psi_k}\right)\dot{\psi}_k = \frac{2\pi}{T}\sum_{k=1}^{N}\left(\frac{\partial\mathcal{W}}{\partial\psi_k}\right)\rho_d s_k^{-1}\zeta_k. \tag{20}$$

Note that

$$\frac{\partial\mathcal{W}}{\partial\psi_k} = \langle ie^{i\psi_k}, \mathcal{L}_k e^{i\boldsymbol{\psi}}\rangle = -\sum_{j\in\mathcal{N}_k}\sin(\psi_j - \psi_k), \tag{21}$$

where, $\mathcal{L}_k$ is the k^{th} row of the Laplacian $\mathcal{L}$. Thus,

$$\dot{\mathcal{W}}(\boldsymbol{\psi}) = \frac{2\pi}{T}\sum_{k=1}^{N}\langle ie^{i\psi_k}, \mathcal{L}_k e^{i\boldsymbol{\psi}}\rangle\rho_d s_k^{-1}\zeta_k. \tag{22}$$

IV. Control Design

This section proposes the stabilizing controllers to achieve trajectory-constrained temporal synchronized and balanced phase patterns (in the sense of Definition 2) in a uniform flowfield as described in Subsection II-B.

Theorem 1. *Consider the vehicle model* (4) *and assume that the initial states of the vehicles are given such that the condition $|e_k(0)| < \delta$ satisfies for all k, where e_k and δ are defined as above. Let the vehicles be governed by the control law*

$$\zeta_k = \omega_k\left(1 + \left[\kappa s_k\frac{\langle r_k - c_d, e^{i\gamma_k}\rangle}{\delta^2 - |e_k|^2} + K\langle ie^{i\psi_k}, \mathcal{L}_k e^{i\boldsymbol{\psi}}\rangle\right]\right), \tag{23}$$

where, $\rho_d > 0, \omega_k = s_k/\rho_d$, and κ and K are the controller gains. Then, we have the following:

(i) *If $K > 0$ and $\kappa > 0$, all the vehicles asymptotically converge to a circular formation in which each vehicle moves around the desired circle of radius ρ_d and center c_d in temporal phase balancing.*

(ii) *If $K < 0$ and $\kappa > 0$, all the vehicles asymptotically converge to a circular formation in which each vehicle moves around the desired circle of radius ρ_d and center c_d in temporal phase synchronization.*

(iii) *Moreover, the trajectories of the vehicles remain bounded within the circular region $|r_k(t) - c_d| <$*

$(\delta + \rho_d)$ *centered at* c_d *for all* $t \geq 0$ *in both cases (i) and (ii) above.*

Proof. The proof is separately given for the each part.

(i) Consider the following composite potential function

$$\mathcal{V}_1 = \kappa \mathcal{S}(\boldsymbol{r}, \boldsymbol{\gamma}) + K \frac{T}{2\pi} \left(\frac{N}{2} \sigma_{\max} - \mathcal{W}(\boldsymbol{\psi}) \right); \quad \kappa, K > 0, \tag{24}$$

which is a valid Lyapunov function as $0 \leq \mathcal{W}(\boldsymbol{\psi}) \leq \frac{N}{2}\sigma_{\max}$ (Lemma 2). Taking the time derivative of $\mathcal{V}_1$ along the trajectories of the system (4), yields

$$\dot{\mathcal{V}}_1 = \sum_{k=1}^{N} \Bigg[\kappa s_k \frac{\langle r_k - c_d, e^{i\gamma_k} \rangle}{\delta^2 - |e_k|^2} \left(1 - \frac{\zeta_k}{\omega_k} \right) - K \langle i e^{i\psi_k}, \mathcal{L}_k e^{i\boldsymbol{\psi}} \rangle \frac{\zeta_k}{\omega_k} \Bigg] \tag{25}$$

From (21), one can easily check that the gradient vector $\partial \mathcal{W}/\partial \psi_k$ satisfies

$$\sum_{k=1}^{N} \frac{\partial \mathcal{W}}{\partial \psi_k} = -\sum_{k=1}^{N} \sum_{j \in \mathcal{N}_k} \sin(\psi_j - \psi_k) = 0,$$

by using which and then substituting for the control law (23) in (25), yields

$$\dot{\mathcal{V}}_1 = -\sum_{k=1}^{N} \left[\kappa s_k \frac{\langle r_k - c_d, e^{i\gamma_k} \rangle}{\delta^2 - |e_k|^2} + K \langle i e^{i\psi_k}, \mathcal{L}_k e^{i\boldsymbol{\psi}} \rangle \right] \leq 0,$$

which implies that $\mathcal{V}_1(\boldsymbol{r}, \boldsymbol{\gamma})$ is non-increasing along the trajectories of (4), that is, $\mathcal{V}_1(\boldsymbol{r}, \boldsymbol{\gamma}) \leq \mathcal{V}_1(\boldsymbol{r}(0), \boldsymbol{\gamma}(0))$, provided $\mathcal{V}_1(\boldsymbol{r}(0), \boldsymbol{\gamma}(0))$ is bounded. However, since $\mathcal{S}(\boldsymbol{r}, \boldsymbol{\gamma})$ is positive-definite and continuously differentiable in the set $|e_k(t)| < \delta$, $\mathcal{V}_1(\boldsymbol{r}(0), \boldsymbol{\gamma}(0))$ is finite and positive for the *given* initial conditions in the set $|e_k(0)| < \delta, \forall k$. Thus, by using the LaSalles' invariance principle, it can be concluded that all the solutions lies in the largest invariant set Θ, contained in the set where $\{\dot{\mathcal{V}}_1 = 0\}$. Note that $\dot{\mathcal{V}}_1 = 0$ implies

$$\kappa s_k \frac{\langle r_k - c_d, e^{i\gamma_k} \rangle}{\delta^2 - |e_k|^2} + K \langle i e^{i\psi_k}, \mathcal{L}_k e^{i\boldsymbol{\psi}} \rangle = 0, \tag{26}$$

for all $k = 1, \ldots, N$. According to (23), in the set Θ, $\zeta_k = \omega_k = s_k/\rho_d, \forall k$, that is, all the vehicles move around circular orbit of radius ρ_d and fixed center with angular speeds ω_k. Moreover, $\dot{\psi}_k = 2\pi/T$ for all k, which implies that $\dot{\mathcal{W}} = 0$, using (22) and (21). Thus, $\mathcal{W}(\boldsymbol{\psi})$ is constant and hence $\partial \mathcal{W}/\partial \psi_k = \langle i e^{i\psi_k}, \mathcal{L}_k e^{i\boldsymbol{\psi}} \rangle = 0$ for all $k = 1, \ldots, N$, in the set Θ. Consequently, in the set Θ, (26) reduces to

$$\langle r_k - c_d, e^{i\gamma_k} \rangle = 0, \tag{27}$$

as $s_k > 0$ for all k. It is easy to verify that (27) is satisfied only if (13) holds, that is, all the vehicles asymptotically converge on a common circle centered at c_d and has radius ρ_d. Moreover, since $\mathcal{V}_1(\boldsymbol{r}, \boldsymbol{\gamma})$ is decreasing, $\frac{N}{2}\sigma_{\max} - \mathcal{W}(\boldsymbol{\psi})$ also approaches to zero, or in other words, $\mathcal{W}(\boldsymbol{\psi})$ approaches its maximum value, which corresponds to the temporal phase balancing (Lemma 2) on the desired common circle.

(ii) Consider the potential function

$$\mathcal{V}_2(\boldsymbol{r}, \boldsymbol{\gamma}) = \kappa \mathcal{S}(\boldsymbol{r}, \boldsymbol{\gamma}) - K \frac{T}{2\pi} \mathcal{W}(\boldsymbol{\psi})); \kappa > 0, K < 0. \tag{28}$$

The time derivative of the potential $\mathcal{V}_2(\boldsymbol{r}, \boldsymbol{\gamma})$ along system dynamics (4), under control (23), results in

$$\dot{\mathcal{V}}_2 = -\sum_{k=1}^{N} \left[\kappa s_k \frac{\langle r_k - c_d, e^{i\gamma_k} \rangle}{\delta^2 - |e_k|^2} + K \langle i e^{i\psi_k}, \mathcal{L}_k e^{i\boldsymbol{\psi}} \rangle \right] \leq 0.$$

Since $\dot{\mathcal{V}}_2 = \dot{\mathcal{V}}_1$, the rest of the proof follows the same steps as case (i) above. Moreover, the proof of part (iii) directly follows from Lemma 1 and avoided for brevity. □

Given the controls ζ_k in the inertial frame, one can further obtains the actual applied control u_k in (3b). We obtain this expression in the following corollary.

Corollary 1. *The control* u_k *in* (3b) *is given by*

$$u_k = \frac{\omega_k \left(1 + \left[\kappa s_k \frac{\langle r_k - c_d, e^{i\gamma_k} \rangle}{\delta^2 - |e_k|^2} + K \langle i e^{i\psi_k}, \mathcal{L}_k e^{i\boldsymbol{\psi}} \rangle \right] \right)}{1 - \lambda s_k^{-1} \cos(\mu - \gamma_k)}.$$

Proof. Substituting (23) in (10) proves the result. □

Next, we obtain a restricted bounds on the absolute values of the errors and the vehicles' trajectories in the following theorem. We also obtain bounds on the relative temporal phasors of the vehicles.

Theorem 2 (*Temporal Phase Balancing*)**.** *Consider the closed loop system model* (4)*, under control* (23) *with* $\kappa > 0, K > 0$*, and assume that the initial states of the vehicles are given such that the condition* $|e_k(0)| < \delta$ *is satisfied for all* k*, where* e_k *and* δ *are defined above. Then the following properties hold.*

(i) *The absolute values of the error signals* e_k*, and the trajectories* r_k*, for all* $k = 1, \ldots, N$*, are bounded by*

$$|e_k| \leq \delta \sqrt{1 - e^{-\frac{2\mathcal{V}_1(\boldsymbol{r}(0), \boldsymbol{\gamma}(0))}{\kappa}}};$$
$$|r_k - c_d| \leq \rho_d + \delta \sqrt{1 - e^{-\frac{2\mathcal{V}_1(\boldsymbol{r}(0), \boldsymbol{\gamma}(0))}{\kappa}}}.$$

(ii) *The squared summation of the relative temporal phasors belongs to the compact set*

$$\sum_{\{j,k\} \in \mathcal{E}} |e^{i\psi_j} - e^{i\psi_k}|^2 \in [\chi_{min}, \chi_{max}].$$

where, $\chi_{min} = \max\left\{0, \left(N\sigma_{max} - \frac{4\pi \mathcal{V}_1(\boldsymbol{r}(0), \boldsymbol{\gamma}(0))}{KT} \right)\right\}$, $\chi_{max} = N\sigma_{max}$*, and* $\mathcal{V}_1(\boldsymbol{r}, \boldsymbol{\gamma})$ *is defined in* (24)*.*

Theorem 3 (*Temporal Phase Synchronization*)**.** *Consider the closed loop system model* (4)*, under control* (23) *with* $\kappa > 0, K < 0$*, and assume that the initial states of the vehicles are given such that the condition* $|e_k(0)| < \delta$ *is satisfied for all* k*, where* e_k *and* δ *are defined above. Then the following properties hold.*

(i) *The absolute values of the error signals* e_k*, and the trajectories* r_k*, for all* $k = 1, \ldots, N$*, are bounded by*

$$|e_k| \leq \delta \sqrt{1 - e^{-\frac{2\mathcal{V}_2(\boldsymbol{r}(0), \boldsymbol{\gamma}(0))}{\kappa}}};$$
$$|r_k - c_d| \leq \rho_d + \delta \sqrt{1 - e^{-\frac{2\mathcal{V}_2(\boldsymbol{r}(0), \boldsymbol{\gamma}(0))}{\kappa}}}.$$

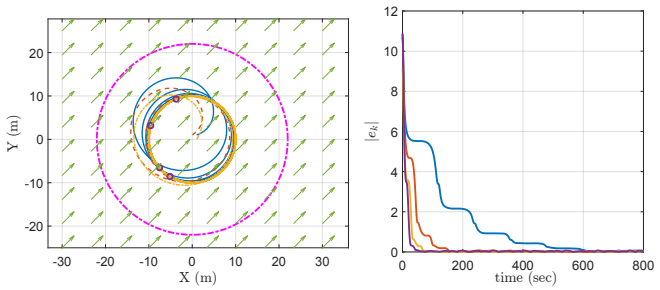

(a) Trajectories (b) Errors

Fig. 2. Trajectories and motion errors for the vehicles under the control (23) with controller gains $\kappa = 5$ and $K = 0.01$.

(ii) *The squared summation of the relative temporal phasors belongs to the compact set*

$$\sum_{\{j,k\}\in\mathcal{E}} |e^{i\psi_j} - e^{i\psi_k}|^2 \in [0, \Gamma],$$

where, $\Gamma = \min\left\{-\frac{4\pi\mathcal{V}_2(\boldsymbol{r}(0),\boldsymbol{\theta}(0))}{KT}, N\sigma_{max}\right\}$*, and* $\mathcal{V}_2(\boldsymbol{r},\boldsymbol{\gamma})$ *is defined in* (28).

The proofs of above theorems are based on the boundedness of the respective Lyapunov functions in temporal phase synchronization and balancing, and are omitted for brevity. The readers may refer [20] for further details.

Example 1. *Consider* $N = 4$ *vehicles with initial positions, heading angles and speeds given by* $\boldsymbol{x}(0) = [1,\ 0,\ 1,\ -1]^T; \boldsymbol{y}(0) = [1,\ 1,\ 0,\ -1]^T; \boldsymbol{\theta}(0) = [0°,\ 30°,\ 60°,\ 90°]^T; \boldsymbol{v} = [1,\ 1.5,\ 2,\ 2.5]^T$*. The flowfield* f *has the magnitude* $\lambda = 0.75$ *in direction* $\mu = 45°$*. The radius and center of the desired circle are* $c_d = (0, 0)$ *and* $\rho_d = 10$*, respectively. The radius of the circular boundary is considered as* $\delta = 12$*. With these given conditions, one can easily verify that the conditions* $|e_k(0)| < \delta$ *is satisfied for all the vehicles. Let the agents are sharing information according to a circulant graph whose Lapacian is given by*

$$\mathcal{L} = \begin{bmatrix} 2 & -1 & 0 & -1 \\ -1 & 2 & -1 & 0 \\ 0 & -1 & 2 & -1 \\ -1 & 0 & -1 & 2 \end{bmatrix}.$$

Figure 2 shows the trajectories and the motion error for the vehicles under the control law (23) with controller gains $\kappa = 5$ and $K = 0.01$. It is clear that all the vehicles converge to the desired circle in temporal phase balancing. The plot for $K < 0$ (temporal phase synchronization) is similar and omitted due to space limitations.

V. Conclusions and Future Work

We investigated collective circular formation control of the unicycle-type vehicles with temporal synchronization and balancing phase arrangements in a uniform time-invariant flowfield. The controllers were designed by using the concept of BLF in composition with temporal phase potential functions that allows the limited information exchange among vehicles. The bounds on the motion and trajectory errors and the relative temporal phasors were derived.

In future, we would like to generalize the problem by considering practical issues such as collision avoidance, saturated and time-delay control, while allowing the vehicle to move around different closed curves (possibly convex).

References

[1] K.-K. Oh, M.-C. Park, and H.-S. Ahn, "A survey of multi-agent formation control," *Automatica*, vol. 53, pp. 424–440, 2015.

[2] I. D. Couzin, J. Krause, R. James, G. D. Ruxton, and N. R. Franks, "Collective memory and spatial sorting in animal groups," *Journal of Theoretical Biology*, vol. 218, no. 1, pp. 1–11, 2002.

[3] N. E. Leonard, D. A. Paley, F. Lekien, R. Sepulchre, D. M. Fratantoni, and R. E. Davis, "Collective motion, sensor networks, and ocean sampling," *Proceedings of the IEEE*, vol. 95, no. 1, pp. 48–74, 2007.

[4] R. Sepulchre, D. A. Paley, and N. E. Leonard, "Stabilization of planar collective motion with limited communication," *IEEE Transactions on Automatic Control*, vol. 53, no. 3, pp. 706–719, 2008.

[5] H.-T. Zhang, Z. Chen, L. Yan, and W. Yu, "Applications of collective circular motion control to multirobot systems," *IEEE Transactions on Control Systems Technology*, vol. 21, no. 4, pp. 1416–1422, 2013.

[6] G. S. Seyboth, J. Wu, J. Qin, C. Yu, and F. Allgöwer, "Collective circular motion of unicycle type vehicles with nonidentical constant velocities," *IEEE Transactions on control of Network Systems*, vol. 1, no. 2, pp. 167–176, 2014.

[7] L. Briñón-Arranz, L. Schenato, and A. Seuret, "Distributed source seeking via a circular formation of agents under communication constraints," *IEEE Transactions on Control of Network Systems*, vol. 3, no. 2, pp. 104–115, 2016.

[8] X. Yu, L. Liu, and G. Feng, "Distributed circular formation control of nonholonomic vehicles without direct distance measurements," *IEEE Transactions on Automatic Control*, vol. 63, no. 8, pp. 2730–2737, 2018.

[9] A. Jain and D. Ghose, "Stabilization of collective motion in synchronized, balanced and splay phase arrangements on a desired circle," in *Proc. of American Control Conference (ACC)*, Chicago, USA, 2015, pp. 731–736.

[10] M. B. Milam, N. Petit, and R. M. Murray, "Constrained trajectory generation for micro-satellite formation flying," in *AIAA Guidance, Navigation and Control Conference*, Montreal, Canada, 2001, pp. 328–333.

[11] C. Peterson and D. A. Paley, "Multivehicle coordination in an estimated time-varying flowfield," *Journal of Guidance, Control, and Dynamics*, vol. 34, no. 1, pp. 177–191, 2011.

[12] A. D. Ames, J. W. Grizzle, and P. Tabuada, "Control barrier function based quadratic programs with application to adaptive cruise control," in *53rd IEEE Conference on Decision and Control (CDC)*, California, USA, 2014, pp. 6271–6278.

[13] M. Z. Romdlony and B. Jayawardhana, "Stabilization with guaranteed safety using control lyapunov–barrier function," *Automatica*, vol. 66, pp. 39–47, 2016.

[14] L. Wang, A. Ames, and M. Egerstedt, "Safety barrier certificates for heterogeneous multi-robot systems," in *Proc. American Control Conference (ACC)*, Boston, USA, 2016, pp. 5213–5218.

[15] D. Panagou, D. M. Stipanović, and P. G. Voulgaris, "Distributed coordination control for multi-robot networks using lyapunov-like barrier functions," *IEEE Transactions on Automatic Control*, vol. 61, no. 3, pp. 617–632, 2016.

[16] P. Glotfelter, J. Cortés, and M. Egerstedt, "Nonsmooth barrier functions with applications to multi-robot systems," *IEEE Control Systems Letters*, vol. 1, no. 2, pp. 310–315, 2017.

[17] D. Han and D. Panagou, "Robust multi-task formation control via parametric lyapunov-like barrier functions," *IEEE Transactions on Automatic Control (Early Access)*, 2019.

[18] K. P. Tee, S. S. Ge, and E. H. Tay, "Barrier lyapunov functions for the control of output-constrained nonlinear systems," *Automatica*, vol. 45, no. 4, pp. 918–927, 2009.

[19] Z.-L. Tang, K. P. Tee, and W. He, "Tangent barrier lyapunov functions for the control of output-constrained nonlinear systems," *3rd IFAC International Conference on Intelligent Controland Automation Science*, vol. 46, no. 20, pp. 449–455, 2013.

[20] A. Jain and D. Ghose, "Trajectory-constrained collective circular motion with different phase arrangements," *Submitted to a Journal*.

[21] ——, "Collective circular motion in synchronized and balanced formations with second-order rotational dynamics," *Communications in Nonlinear Science and Numerical Simulation*, vol. 54, pp. 156–173, 2018.